JOURNAL OF GUIDANCE, CONTROL, AND DYNAMICS
Vol. 17, No. 2, March–April 1994

Computation of Near-Minimum-Time Maneuvers of Flexible Structures by Parameter Optimization

S. R. Vadali,* T. Singh,† and T. Carter‡
Texas A&M University, College Station, Texas 77843

Near-minimum-time attitude maneuvers of space structures as well as ground-based test articles are considered. The switching nature of the controls for rigid-body maneuvers is illustrated using a control cube and a critical control axis. The presence of torque smoothing and, where appropriate, gravitational effects and connections to other bodies are explicitly included in the mathematical models of the systems to be optimized. A maximum fuel consumption constraint is included along with the required terminal conditions on attitude and angular velocities. The switch times, maximum thrust magnitudes, and smoothing parameters are determined using the sequential quadratic programming method for parameter optimization. Results indicating attitude and angular velocity histories, thruster forces, and structural vibrations are presented for three, four, and five switch maneuvers, as well as maneuvers that involve large coasting arcs.

Introduction

OPTIMAL large-angle maneuvering of spacecraft has been a topic of interest for more than a decade.[1–18,21–25] A variety of performance indices based on torque, power, and time have been considered. Except for Refs. 12 and 13, applications to flexible spacecraft models have been limited to single-axis maneuvers. A recent survey article on time-optimal attitude maneuvers is presented in Ref. 18. Solution to the optimization problem usually proceeds by invoking Pontryagin's principle, which leads to a two-point boundary-value problem (TPBVP).[19] This is solved using either direct (gradient) or indirect (shooting) methods. The switch-time optimization algorithm (STO)[20] is a direct method available for the solution of time-optimal control problems. Adaptation of a shooting method to solve time-optimal maneuver problems is given by Li and Bainum.[21]

Bilimoria and Wie[22] considered the specific problem of time-optimal control of a sphere with three orthogonal control inputs, each bounded by ±1. They also restricted their attention to attitude boundary conditions that could otherwise be achieved by single-axis rotations about an Euler axis. Their results show that Euler-axis rotations are not time optimal in general; there are two types of switching sequences: five switches for rotation angles greater than 73 deg and seven switches for angles less than 73 deg. The switches are sequential, i.e., no control switches for the second time before all others switch. Li and Bainum[21] present results for rest-to-rest maneuvers of nearly symmetric spacecraft that show similar behavior. However, for highly unsymmetric spacecraft and arbitrary attitude boundary conditions, the number and sequence of switches are not predictable as they are for spherical bodies. Byers and Vadali[23] and Byers et al.[24] used the STO algorithm to compare the Euler-axis, five-switch, and seven-switch maneuvers for Euler-axis boundary conditions and found that the differences in the maneuver times are insignificant for practical implementations. A suboptimal control strategy was developed in Ref. 23 by assuming a five-switch control sequence and an approximate solution to the Euler parameter differential equation. This switching structure also encompasses the three-switch sequence. This open-loop controller is augmented by a terminal feedback controller in Ref. 24. The presence of singular controls for arbitrary attitude maneuvers was investigated by Kumar and Seywald.[25]

In this paper, near-minimum-time large-angle maneuvers of unsymmetric structures with control inputs that produce interaxis coupling are considered. The specific structure under consideration is the advanced structure technology research experiment (ASTREX) test article (Fig. 1) located in the Phillips Laboratory at Edwards Air Force Base, California. The effect of the number of switches on the maneuver time is determined for near-optimal implementations. A geometric viewpoint using a control cube and

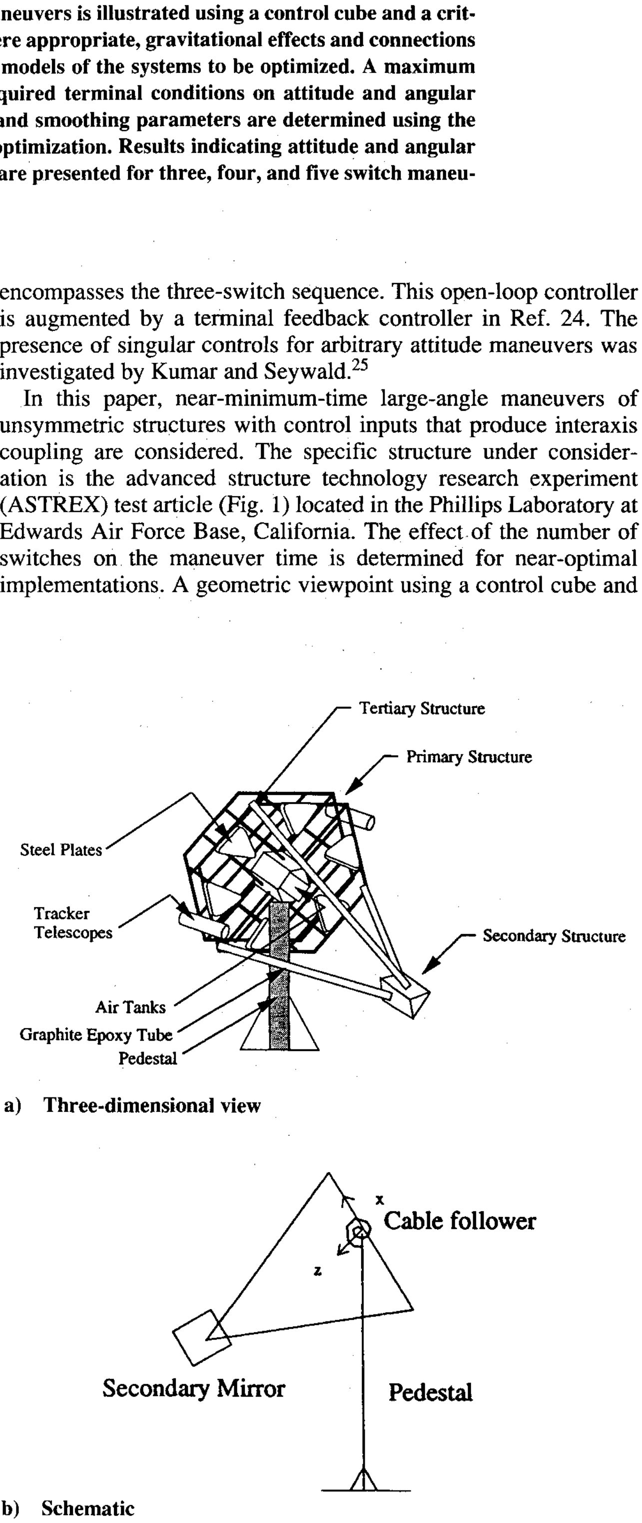

Fig. 1 ASTREX test article.

Received June 12, 1992; presented as Paper 92-4459 at the AIAA Guidance, Navigation, and Control Conference, Hilton Head, SC, Aug. 10–12, 1992; revision received June 21, 1993; accepted for publication June 21, 1993.

*Associate Professor, Aerospace Engineering. Associate Fellow AIAA.

†Postdoctoral Fellow, Aerospace Engineering; currently Assistant Professor, Mechanical and Aerospace Engineering, State University of New York at Buffalo, Buffalo, NY. Member AIAA.

‡Graduate Student, Department of Aerospace Engineering. Student Member AIAA.

Table 1 Thruster data

No.	Thrust, lbf	Location, m	+Thrust direction	Relationship to $\boldsymbol{u}$
1	8	[−1.35 −2.7 −0.25]	[−0.5 0 −0.867]	$8u_1$
2	8	[1.35 −2.7 −0.25]	[0.5 0 0.867]	$-8u_2$
3	8	[1.35 2.7 −0.25]	[−0.5 0 −0.867]	$-8u_1$
4	8	[−1.35 2.7 −0.25]	[0.5 0 0.867]	$8u_2$
5	8	[−2.83 0 −0.05]	[−0.5 0 −0.867]	$-8u_3$
6	8	[2.83 0 −0.05]	[0.5 0 0.867]	$-8u_3$
7	200	[−1.35 −2.55 −0.25]	[0.5 0 0.867]	$200u_2$
8	200	[−1.35 −2.55 −0.25]	[−0.5 0 −0.867]	$200u_1$
9	200	[1.35 2.55 −0.25]	[−0.5 0 −0.867]	$-200u_1$
10	200	[1.35 2.55 −0.25]	[0.5 0 0.867]	$-200u_2$

a critical control axis provides good initial guesses for the controls and also makes visualization of the switching sequence easy. The switch times, maximum thrust magnitudes, and smoothing parameters are optimized using the sequential quadratic programming (SQP) technique. Optimization of parameters is conceptually simpler than the solution of the TPBVP in the state-costate space. Torque smoothing is included in the mathematical model of the system to attenuate the high-frequency content in the bang-bang control profiles. A maximum fuel consumption constraint is also included to account for limited fuel available for the thrusters. Additional dynamics due to the connection of the primary structure to a nonmaneuvering pedestal are also included where appropriate. Simulation results for three-, four-, and five-switch maneuvers, as well as maneuvers involving significant coasting arcs, are presented. The maneuvers are compared in terms of maneuver time, structural vibrations, and implementation issues.

Mathematical Models of the ASTREX Test Article

The ASTREX test article is designed to float on a pedestal using a two-axis airbearing system. The primary actuators are 14 thrusters located on the hexagonal primary mirror as shown in Fig. 2. Of the 14 actuators, 6 are 8-lbf bidirectional thrusters and 8 are 200-lbf unidirectional thrusters. The 200-lbf thrusters will be operated as four bidirectional thrusters. All of the thrusters can be throttled. The locations of the thrusters with respect to the pivot point and their magnitudes are given in Table 1. These thrusters are canted, as shown in Fig. 2, so that they create moments about all of the three primary axes of the structure. The position vector of the center of mass of the structure with respect to the pivot point is (in meters) [−0.0035, 0.00025, −0.00017]. Hence gravitational moments have to be accounted for. The connection of the primary test article to the airbearing table and the dynamics of the cable follower are modeled by two springs, one in the pitch axis of an intermediate frame and the other in the roll axis of the body axis.

For many applications involving large slew motions, a rigid body assumption is invoked for a preliminary control design as will be done here. The moment of inertia matrix with respect to the basic coordinate system at the pivot point (in kilograms-meters squared) as follows:

$$\begin{bmatrix} 22239.3 & -14.63 & -211.02 \\ -14.63 & 15680.13 & -8.164 \\ -211.02 & -8.164 & 22270.42 \end{bmatrix}$$

The total mass of the structure is 5091.9 kg. The attitude is measured by angle-encoding devices and converted to Euler parameters by the onboard control and data acquisition computer. The differential equations for the time rate of change of these parameters is given by

$$\dot{\beta} = {}^1\!/\!_2 [G(\omega)]\beta \tag{1}$$

where ω (ω_1, ω_2, ω_3) is the angular velocity vector with the components in a body-fixed axis system and

$$[G(\omega)] = \begin{bmatrix} 0 & -\omega_1 & -\omega_2 & -\omega_3 \\ \omega_1 & 0 & \omega_3 & -\omega_2 \\ \omega_2 & -\omega_3 & 0 & \omega_1 \\ \omega_3 & \omega_2 & -\omega_1 & 0 \end{bmatrix}$$

The equation of rotational motion for a rigid body under the action of thrust moments only is

$$I\dot{\omega} = -\tilde{\omega}I\omega + Bu \tag{2}$$

where I is the inertia matrix, and $\tilde{\omega}$ is the angular velocity cross-product operator. Matrix B is the control influence matrix. It is scaled to include the thrust saturation value of the individual thrusters as well as their moment arms. Hence, the individual elements of $\boldsymbol{u}$ are bounded between ± 1.

The thrusters are fired in pairs so as not to cause any translation. When the six 8-lbf thrusters are used, matrix B is given (in Newton- meter) as follows:

$$\begin{bmatrix} 167.14 & 167.14 & 0 \\ -83.21 & -83.21 & 0 \\ -96.5 & -96.5 & 201.17 \end{bmatrix}$$

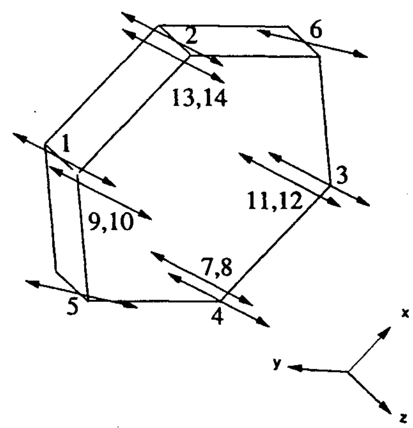

Fig. 2 Orientation of thrusters.

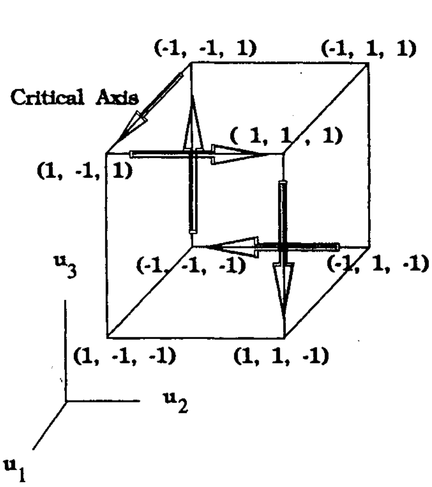

Fig. 3 Switching pattern for a five-switch maneuver.

When a combination of the eight 200-lbf thrusters and two 8-lbf roll thrusters are used, B is

$$\begin{bmatrix} 3924.08 & 3924.08 & 0 \\ -2080.31 & 2080.31 & 0 \\ -2265.57 & -2265.57 & 201.17 \end{bmatrix}$$

The test article is so arranged on the airbearing system that the resting attitude corresponds to a 30-deg pitch-down orientation.

Equation (2) has to be modified to include the spring and gravitational moments. The gravitational moment M_g is given by

$$M_g = \boldsymbol{r} \times (-mg) C_1 \tag{3}$$

where $\boldsymbol{r}$ is the position vector of the center of gravity of the test article with respect to the pivot point, m is the mass of the structure, g is the acceleration due to gravity, and C_1 is the first column of the direction cosine matrix describing the attitude of the test article with respect to the inertial coordinate system. The moment due to the springs M_s is given by

$$M_s = -k_p \begin{Bmatrix} \sin\theta_3 \\ \cos\theta_3 \\ 0 \end{Bmatrix} \left(\theta_2 + \frac{\pi}{6}\right) - k_r \begin{Bmatrix} 0 \\ 0 \\ 1 \end{Bmatrix} \theta_3 \tag{4}$$

where θ_1, θ_2, and θ_3 are the yaw, pitch, and roll Euler angles, respectively; and k_p and k_r are, respectively, the pitch and roll spring constants. Note that the pitch spring is centered at -30 deg. Neglecting the flexibility of the support column, the equation of motion of the test article is given by the following equation:

$$I\dot{\omega} = -\tilde{\omega}I\omega + M_g + M_s + B\boldsymbol{u} \tag{5}$$

A NASTRAN finite element model[26] of ASTREX is also available. It consists of approximately 400 nodes and 900 elements. The first two structural modes at approximately 3.4 and 4.8 Hz are pedestal bending modes. The first bending mode of the truss structure is at 10.25 Hz. The output of this program is used to generate a linearized system description in the MATRIX_X environment. Control inputs, actuators, and sensors locations can be provided and vibration and line-of-sight error estimates can be obtained using this model.

Observations on the Switching Structure

To get an understanding of the switching pattern, some approximations are made. Given the initial and final attitudes, the equivalent Euler axis l and the principal angle θ_f are computed with respect to the initial body frame. Without loss of generality, the Euler axis is constrained to lie in the positive half-space $\in R_3$. The gyroscopic terms in the equations of motion are neglected. Assuming that the motion indeed is an Euler rotation, the following approximate equation is written:

$$B^{-1}Il\ddot{\theta} = \boldsymbol{u} \tag{6}$$

where $\ddot{\theta}$ represents the angular acceleration. The three scalar equations implicit in Eq. (6) can be solved as uncoupled single-axis minimum-time rest-to-rest maneuver equations with the usual saturation constraints on the control variables. The axis that requires the greatest time to complete the synthetic maneuver is termed the critical control axis. This axis can be easily identified by looking for the absolute maximum element in the vector $B^{-1}Il$. Since there are three independent controls and they take on values of either +1 or -1 (excluding singular controls), all possible control states at any given instant can be easily located on a cube as shown in Fig. 3. Once the critical axis is identified, the following pattern emerges from analyzing the results of Refs. 21–24:

1) If axis i is the designated critical axis, then the control sequence is such that the control trajectory lies primarily on the faces of the cube to which the critical axis is normal.

2) If the principal angle of rotation is positive (negative), then the control trajectory follows a counterclockwise (clockwise) path starting on the near (far) face looking opposite the arrow indicating the positive half-axis.

3) There is only a single switch of the critical axis control.

4) After the critical axis switch, the control trajectory follows a counterclockwise (clockwise) path on the far (near) face looking opposite the arrow indicating the positive half-axis for positive (negative) principal rotation angles.

A five-switch maneuver with u_1 being the critical control is depicted in Fig. 3. The Euler rotation for this example is negative. The most important observation is the single critical axis switch. For spherical bodies, this happens exactly at the middle of the time interval. Gyroscopic effects destroy the symmetry. Any general maneuver can be performed using three switches, although the saturation levels for the three controls might be different. As more switches are allowed in the noncritical axes, in the nonsingular case, the controls reach their specified saturation limits, and the maneuver time approaches the optimal value. Using the cube, the four possibilities for the initial control can be identified for any maneuver. This reduces the search space by more than 50%.

Torque Shaping

Since present day spacecraft are becoming increasingly fragile and flexible, smooth torque profiles are desirable and, in some cases, mandatory. Torque-shaping techniques using a multiplier function to shape the controls during the initial and final phases of a maneuver have been discussed in Refs. 3, 14, and 16. Approximations to the sharp control switches are made to shape the control during the intermediate phases of the maneuver. As in Thompson et al.,[14] a multiplier function $m_1(t)$ is designed as follows:

$$m_1(t) = \tau^2(3 - 2\tau); \qquad \tau = t/T_R, \qquad t \le T_R$$

$$m_1(t) = 1, \qquad T_R \le t \le 1 - T_R \tag{7}$$

$$m_1(t) = 1 - \tau^2(3 - 2\tau); \quad \tau = [t - (1 - T_R)]/T_R, \quad t > 1 - T_R$$

The rise time T_R is selected to control sharpness (frequency content) of the multiplier function. The final time is normalized to 1.

The sign function used to represent the sharp switches in minimum-time control problems is approximated as follows:

$$u_i = \text{sign}(s_i) \approx 2/\pi \tan^{-1}(s_i/\alpha_i) \tag{8}$$

where s_i is the switching function, and the parameter α_i controls the smoothness of the approximation. The parameters T_R and α_i can either be chosen a priori or be optimized. It is prudent to optimize these parameters only when a fuel constraint is also included.

When a fuel constraint is active, there is a possibility of having coasting arcs. To explore this possibility, we consider another multiplier:

$$m_2(\tau) = \tau^2(3 - 2\tau), \qquad t \le t_1, \qquad \tau = t/t_1$$

$$m_2(\tau) = (2 - \tau)^2(2\tau - 1), \qquad t_1 \le t \le 2t_1, \qquad \tau = t/t_1$$

$$m_2(\tau) = -\tau^2(3 - 2\tau), \quad (1 - 2t_1) \le t \le (1 - t_1), \quad \tau = (t + 2t_1 - 1)/t_1$$

$$m_2(\tau) = -(2 - \tau)^2(2\tau - 1), \quad (1 - t_1) \le t \le 1, \quad \tau = (t + 2t_1 - 1)/t_1$$

$$m_2(\tau) = 0, \text{otherwise} \tag{9}$$

This function is zero except during the intervals $[0, 2t_1]$ and $[1 - 2t_1, 1]$. During these intervals it is approximately impulsive in nature; the smaller the value of t_1, the closer the approximation. When using this function, one needs to optimize the maximum control magnitude and, if desired, the parameter t_1 for each control. Note that $t_1 \leq 0.25$.

Fuel Constraint

At present there are two air tanks to feed the thrusters. The capacity of each tank is 4 ft^3 at a maximum pressure of 500 psi. Assuming a linear relationship between pressure drop Δp in the tanks and volume of air consumed, we can write the following equation:

$$\text{air volume} = 2(\text{tank capacity})\,\Delta p/p_{at} \tag{10}$$

where p_{at} is the atmospheric pressure. Assuming a pressure drop of 300 psi, the air capacity is conservatively estimated to be 160 ft^3. The air volume flow rate $\dot{v}$ is given by the following relationship:

$$\dot{v} = 14\left(\sum_{i=1}^{10}|T_i|\right)\text{ft}^3/\text{min} \tag{11}$$

where T_i is the thrust of each thruster. Equation (11) is integrated over the maneuver time to obtain the volume of air used, which is equivalent to the fuel consumed.

Sensitivity and Parameter Optimization

The problem of finding the maximum control magnitudes, switch times, and smoothing parameters subject to various constraints can be cast as a parameter optimization problem. Consider the following formulation:

Minimize $J = {}^1/_2\, p_0^2$, subject to

$$\dot{x} = f[x, u(p), t]\,p_0; \qquad t \in (0, 1) \tag{12}$$

$$x(1) = x_f \tag{13}$$

$$g(p_i) \geq 0 \tag{14}$$

$$p_{l_i} \leq p_i \leq p_{u_i}; \qquad i = 0, \ldots, n_p \tag{15}$$

where p_0, the final time, and p are $n_p + 1$ parameters to be selected; p_{li} and p_{ui} are, respectively, the lower and upper bounds on the parameters. The state terminal boundary conditions are equality constraints. Since the four Euler parameters are not mutually independent, only the last three are constrained at the final time; β_0 is left free. The control saturation constraints, fuel constraints, and the constraints on the smoothing parameters are inequality constraints. The vector p includes the peak values of the three controls, the switch times, and the smoothing parameters. As an example, a smooth control with two switches is parameterized as follows:

$$u = -m_1(t)p_1(2/\pi)\tan^{-1}[(t - p_2)(t - p_3)/\alpha] \tag{16}$$

The formulation allows many different types of control structures, including bang-bang controls. A two-switch bang-bang profile is incorporated as follows:

$$u = -p_1\,\text{sign}[(t - p_2)(t - p_3)] \tag{17}$$

This problem is a general nonlinear programming problem. One way to solve this problem is through the use of SQP.[27] In this paper, the results were obtained using the codes DQPROG and DNCONF available in the IMSL[28] library.

To mechanize the process, we need to calculate the sensitivity[29] of the final states to the individual parameters. These quantities can either be obtained by finite differencing or by numerical integration of the sensitivity differential equations. Both methods have been used for verification of the results. The latter procedure is outlined next.

The solution to Eq. (12) at the final time can be written as

$$x(1) = x(0) + p_0\int_0^1 \{f[x, u(p), t]\}\,dt \tag{18}$$

Defining $\partial x/\partial p_0 = v_0$ and $\partial x/\partial p = V$ as the sensitivity functions, we can give their final values by the following equations:

$$v_0(1) = \int_0^1 \left\{f[x, u(p), t] + p_0\left[\frac{\partial f}{\partial x}v_0(t)\right]\right\}dt \tag{19}$$

$$V(1) = p_0\int_0^1 \left[\frac{\partial f}{\partial x}V(t) + \frac{\partial f}{\partial p}\right]dt \tag{20}$$

Equations (19) and (20) are converted to differential equations to evaluate the sensitivity functions. For bang-bang controls, certain useful relationships can be developed to evaluate sensitivity functions. For Eq. (17), assuming $p_2 < p_3$, the following formulas apply:

$$\int_0^1 \frac{\partial u}{\partial p_1}\,d\tau = 2(p_3 - p_2) - 1$$

$$\int_0^1 \frac{\partial u}{\partial p_2}\,d\tau = -2p_1$$

$$\int_0^1 \frac{\partial u}{\partial p_3}\,d\tau = 2p_1$$

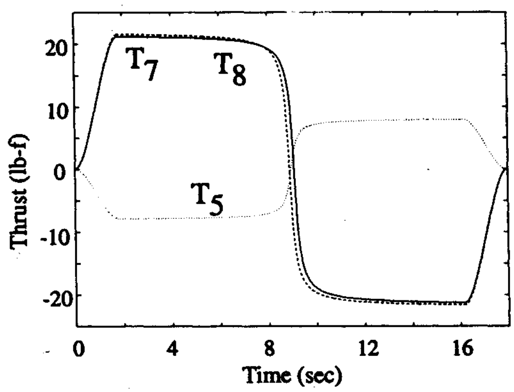

Fig. 4 Three-switch smooth maneuver (200/8 lbf).

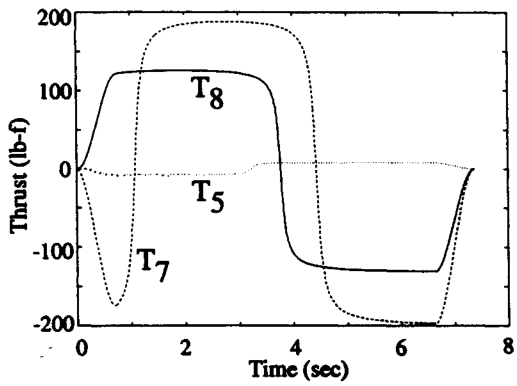

Fig. 5 Four-switch smooth maneuver (200/8 lbf).

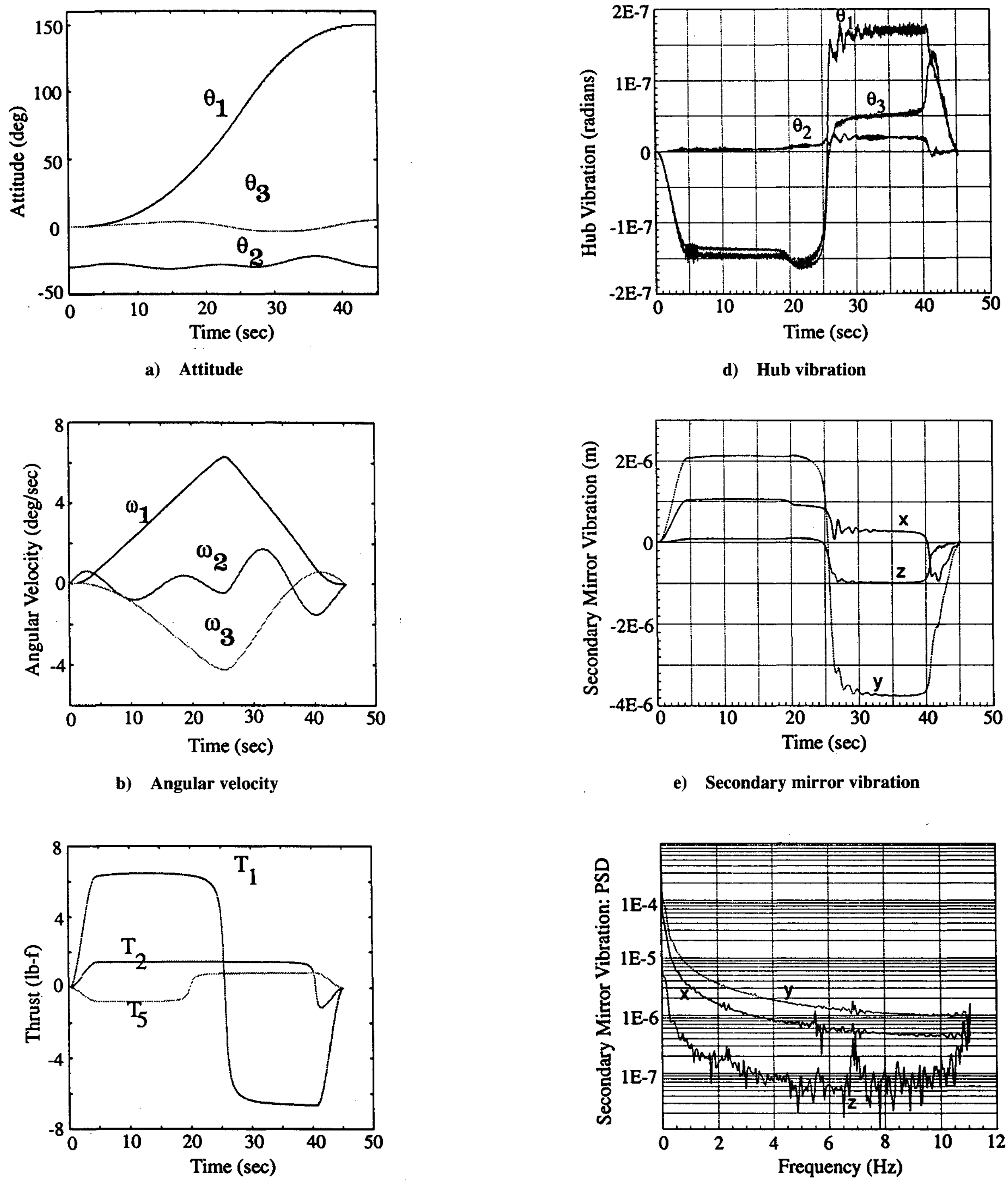

Fig. 6 Three-switch smooth maneuver (8 lbf).

Numerical Examples

Two types of rest-to-rest maneuvers are considered, one for the ASTREX test article under the influence of thrust moments only [Eq. (2)] and the other for the ground-based experiment with all of the dynamic effects and constraints discussed earlier.

Maneuvers of the Floating Test Article

The inertia matrix for these examples is referenced to the center of mass of the test article. The initial Euler angles are [0 −30 0 deg], and the final angles are [150 −10 5 deg]. The smoothing parameters selected for the maneuvers are $\alpha_i = 0.01$ if one switch is allowed, and $\alpha_i = 0.005$ if two switches are allowed. A value of $T_R = 0.1$ is used throughout. For the boundary conditions chosen, u_2 is the critical control when the 8-lbf thrusters are used; u_3 is the critical control when the 200/8-lbf thruster combination is used. The fuel constraint is not imposed here.

Figure 4 shows the thrust profiles for a smooth three-switch maneuver using the 200/8-lbf thruster combination. The maximum values of the nondimensional controls $u_{1_{max}}$, $u_{2_{max}}$, and $u_{3_{max}}$ are 0.108, 0.11, and 1, respectively, and the corresponding nondimensional switch times are 0.505, 0.495, and 0.498, respectively. Figure 5 shows the thrust profiles for a four-switch maneuver. The effect of the number of switches on the maneuver time is dramatically illustrated in these figures. It is clear that restricting the number of switches to three forces the 200-lbf thrusters to operate at 20-lbf levels. The addition of one more switch allows them to operate at much higher levels. The maximum values of the nondimensional controls $u_{1_{max}}$, $u_{2_{max}}$, and $u_{3_{max}}$ are 0.66, 1, and 1, respectively, and the corresponding nondimensional switch times

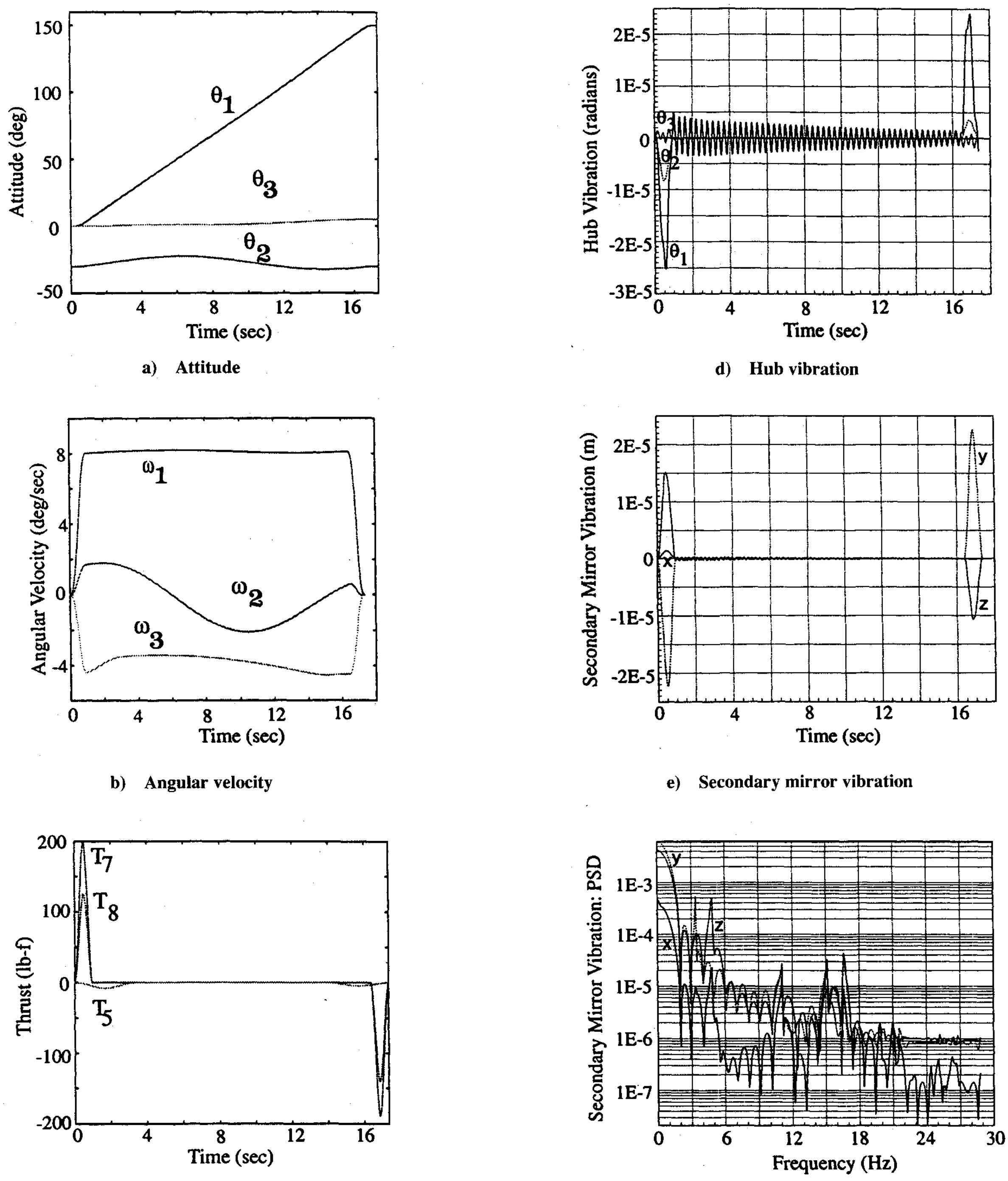

a) **Attitude**
b) **Angular velocity**
c) **Thruster profile**
d) **Hub vibration**
e) **Secondary mirror vibration**
f) **Secondary mirror vibration: PSD**

Fig. 7 Thrust-coast-thrust maneuver (200/8 lbf).

are 0.5, 0.15 (and 0.59), and 0.43, respectively. The maneuver time in Fig. 4 is 7.3 s compared with 18 s in Fig. 5. It is also interesting to observe that the controls u_i behave as predicted by the control-cube hypothesis. Although five switches were allowed, the solution only required four switches. Thrust magnitudes for three of the thrusters are shown in the figures, as the others can be deduced from these using Table 1.

Unfortunately, the test article is allowed to have a maximum slew rate of 10 deg/s in each axis, and the fuel consumed during the maneuvers depicted in Figs. 4 and 5 exceeds the allowable limit. The next set of maneuvers are for the ground-based test article for which the fuel constraint is included.

Maneuvers of the Ground-Based Test Article

For these simulations, the pitch and roll springs are assumed to have spring constants of 2000 and 1000 Nm, respectively. The initial Euler angles in degrees are [0 −30 0], and the final attitude is [150 −30 5 deg]. For these boundary conditions, u_1 is critical for the two types of thruster combinations. The smoothing parameters are also the same as before.

Figure 6 shows the maneuver with the 8-lbf thrusters. The maneuver time is quite large (45.2 s) as the thrust levels are below 6 lbf. Although six switches were allowed, the solution required three switches only. Information regarding the vibrations of the hub and the secondary mirror are also included. This was obtained by applying the open-loop thrust profiles to the finite element model of the test article. It is interesting to note that thruster 2 (and 4) switches late in the maneuver and also the angular velocity constraint is not violated. The maximum values of the nondimensional controls $u_{1_{max}}$, $u_{2_{max}}$, and $u_{3_{max}}$ are 0.84, 0.18, and 0.104, respectively, and the corresponding nondimensional switch times are 0.57, 0.9, and 0.44, respectively.

Figure 7 shows the same maneuver with the 200/8-lbf thrusters operating in a near-impulsive mode. The fuel constraint is active and the smoothing parameters t_1 for the thrusters are optimized. The maneuver time is quite reasonable (16.86 s), as well as the structural vibrations. It is clear that the pedestal bending modes dominate the vibration response. The initial and final peak control magnitudes $u_{1_{\max}}$, $u_{2_{\max}}$, and $u_{3_{\max}}$ are 0.64, −0.75, and 1 and −0.93, 0.69, and 0.16, respectively. The corresponding nondimensional smoothing parameters t_1 are 0.03, 0.03, and 0.1, respectively.

Conclusions

A parameter optimization method is presented for computing near-minimum-time maneuvers of space structures. Torque-smoothing devices and additional dynamics due to interbody connections are explicitly incorporated in the mathematical models. The present method avoids the formulation of an optimal control problem and the associated two-point boundary-value problem. Results indicate that, for large maneuvers without fuel constraints, dramatic improvements in the maneuver times can be achieved by allowing more than three switches (one for each control). When the fuel constraint is active, it is better to use the thrusters in a near-impulsive, thrust-coast-thrust mode rather than a reduced-thrust bang-bang mode. The maneuvers presented are not Euler rotations. The thrust profiles are easy to implement, and the structural vibrations are quite reasonable during maneuvers.

Acknowledgments

This research was performed under the NASA/Department of Defense Control-Structure-Interaction Guest Investigator Program (Contract NAS1-19373). The authors are grateful to Alok Das and Derek Cossey of the Air Force Phillips Laboratory for their input. The efforts of N. S. Abhyankar of DYNACS, Inc., in providing technical data on the ASTREX test article are well appreciated. The support of the Texas Higher Education Coordinating Board through the ATP Grant 999903-264 is gratefully acknowledged.

References

[1]Junkins, J. L., and Turner, J. D., *Optimal Spacecraft Rotational Maneuvers,* Elsevier, Amsterdam, The Netherlands, 1985.

[2]Dwyer, T. A. W., III, "Exact Nonlinear Control of Large Angle Rotational Maneuvers," *IEEE Transactions on Automatic Control,* Vol. AC-29, No. 9, 1984, pp. 769–774.

[3]Vadali, S. R., and Junkins J. L., "Optimal Open Loop and Stable Feedback Control of Rigid Spacecraft Attitude Maneuvers," *The Journal of Astronautical Sciences,* Vol. 32, No. 2, 1984, pp. 105–122.

[4]Skaar, S. B., and Kraige, L. G., "Large-Angle Spacecraft Attitude Maneuvers Using an Optimal Reaction Wheel Power Criterion," *The Journal of Astronautical Sciences,* Vol. 32, No. 1, 1984, pp. 47–62.

[5]Carrington, C. K., and Junkins, J. L., "Optimal Nonlinear Feedback Control of Spacecraft Attitude Maneuvers," *Journal of Guidance, Control, and Dynamics,* Vol. 9, No.1, 1986, pp. 99–107.

[6]Lin, Y. Y., and Kraige, L. G., "Enhanced Techniques for Solving the Two-Point Boundary-Value Problem Associated with the Optimal Attitude Control of Spacecraft," *The Journal of Astronautical Sciences,* Vol. 37, No. 1, 1989, pp. 1–16.

[7]Redding, D. C., and Adams, N. J., "Optimized Rotation-Axis Attitude Maneuver Controller for the Space Shuttle Orbiter," *Journal of Guidance, Control, and Dynamics,* Vol. 9, No. 2, 1987, pp. 4–13.

[8]Etter, J. R., "A Solution of the Time Optimal Euler Rotation Problem," AIAA Guidance, Navigation, and Control Conference, AIAA Paper 89-3601-CP, Boston, MA, Aug. 1989.

[9]Li, F., and Bainum, P.M., "Numerical Approach for Solving Rigid Spacecraft Minimum Time Attitude Maneuvers," *Journal of Guidance, Control, and Dynamics,* Vol. 13, No. 1, 1990, pp. 38–45.

[10]Breakwell, J. A., "Optimal Feedback Slewing of Flexible Spacecraft," *Journal of Guidance, Control, and Dynamics,* Vol. 4, No. 5, 1981, pp. 472–479.

[11]Skaar, S. B., Tang, L., and Yalda-Mooshabad, I., "On-Off Attitude Control of Flexible Satellites," *Journal of Guidance, Control, and Dynamics,* Vol. 9, No. 4, 1986, pp. 507–510.

[12]Chun, H. M., and Turner, J. D., "Frequency-Shaped Large Angle Maneuvers," *The Journal of Astronautical Sciences,* Vol. 36, No. 3, 1988, pp. 219–244.

[13]Singh, T., and Vadali, S. R., "Input Shaped Control of Three-Dimensional Maneuvers of Flexible Spacecraft," AIAA Guidance, Navigation, and Control Conference, AIAA Paper 92-4455, Hilton Head, SC, Aug. 1992; also *Journal of Guidance, Control, and Dynamics,* Vol. 16, No. 6, 1993, pp. 1061–1068.

[14]Thompson, R. C., Junkins, J. L., and Vadali, S. R., "Near-Minimum Time Open-Loop Slewing of Flexible Vehicles," *Journal of Guidance, Control, and Dynamics,* Vol. 12, No. 1, 1989, pp. 82–88.

[15]Singh, G., Kabamba, P. T., and McClamroch, N. H., "Minimum-Time Maneuvers of Flexible Spacecraft," *Mechanics and Control of Large Space Structures,* edited by J. L. Junkins, AIAA, Washington, DC, 1989, pp. 595–637.

[16]Junkins, J. L., Rahman, Z., and Bang, H., "Near-Minimum-Time Maneuvers of Flexible Vehicles: A Liapunov Control Law Design Method," *Mechanics and Control of Large Space Structures,* edited by J. L. Junkins, AIAA, Washington, DC, 1989, pp. 565–593.

[17]Ben-Asher, J., Burns, J. A., and Cliff, E. M., "Time-Optimal Slewing of Flexible Spacecraft," *Journal of Guidance, Control, and Dynamics,* Vol. 15, No. 2, 1992, pp. 360–367.

[18]Scrivener, S., and Thompson, R. C., "Survey of Time-Optimal Attitude Maneuvers," AAS/AIAA Space Flight Mechanics Meeting, AAS Paper 92-168, Colorado Springs, CO, Feb. 24–26, 1992; also *Journal of Guidance, Control, and Dynamics,* Vol. 17, No. 2, 1994, pp. 225–232.

[19]Bryson, A. E., and Ho, Y.-C., *Applied Optimal Control,* Hemisphere, Washington, DC, 1975.

[20]Meier, E. B., and Bryson, A. E., "Efficient Algorithm for Time Optimal Control of a Two-Link Manipulator," *Journal of Guidance, Control, and Dynamics,* Vol. 13, No. 5, 1990, pp. 859–866.

[21]Li, F., and Bainum, P. M., "An Improved Shooting Method for Solving Minimum-Time Maneuver Problems," American Society of Mechanical Engineers, Winter Annual Meeting, Dallas, TX, Nov. 26–30, 1990.

[22]Bilimoria, K. D., and Wie, B., "Minimum Time Large Angle Reorientation of a Rigid Spacecraft," *Journal of Guidance, Control, and Dynamics,* Vol. 16, No. 3, 1993, pp. 446–452.

[23]Byers, R. M., and Vadali, S. R., "Quasi Closed–Form Solution to the Time-Optimal Rigid Spacecraft Reorientation Problem," *Journal of Guidance, Control, and Dynamics,* Vol. 16, No. 3, 1993, pp. 453–461.

[24]Byers, R. M., Vadali, S. R., and Pollock, T. C., "Feedforward/Feedback Control for Near Time-Optimal Spacecraft Reorientation," AAS/AIAA Astrodynamics Specialist Conference, AAS Paper 91-406, Durango, CO, Aug. 1991.

[25]Kumar, R., and Seywald, H., "Singular Control in Minimum Time Spacecraft Reorientation," AIAA Guidance, Navigation, and Control Conference, AIAA Paper 91-2645, New Orleans, LA, Aug. 1991.

[26]Abhyankar, N. S., and Berg, J. L., "ASTREX Model Information: Supplement to astabcd.mat File," Phillips Lab., Edwards Air Force Base, CA, Aug. 15, 1991.

[27]Gill, P. E., Murray, W., and Wright, M. H., *Practical Optimization,* Academic Press, London, 1981.

[28]"IMSL Math/Library," Edition 1.1, IMSL Inc., Houston, TX, Dec. 1989.

[29]Sage, A. P., and White, C. C., III, *Optimum Systems Control,* Prentice-Hall, Englewood Cliffs, NJ, 1977.